

---

01 Jan 1971

## Absolute Excitation Cross Sections Of He<sup>+</sup> In 20-100-keV He<sup>+</sup>-He Collisions Using Energy-loss Spectrometry

D. R. Schoonover

John T. Park

Missouri University of Science and Technology, parkj@mst.edu

Follow this and additional works at: [https://scholarsmine.mst.edu/phys\\_facwork](https://scholarsmine.mst.edu/phys_facwork)

 Part of the [Physics Commons](#)

---

### Recommended Citation

D. R. Schoonover and J. T. Park, "Absolute Excitation Cross Sections Of He<sup>+</sup> In 20-100-keV He<sup>+</sup>-He Collisions Using Energy-loss Spectrometry," *Physical Review A*, vol. 3, no. 1, pp. 228 - 234, American Physical Society, Jan 1971.

The definitive version is available at <https://doi.org/10.1103/PhysRevA.3.228>

This Article - Journal is brought to you for free and open access by Scholars' Mine. It has been accepted for inclusion in Physics Faculty Research & Creative Works by an authorized administrator of Scholars' Mine. This work is protected by U. S. Copyright Law. Unauthorized use including reproduction for redistribution requires the permission of the copyright holder. For more information, please contact [scholarsmine@mst.edu](mailto:scholarsmine@mst.edu).

## ACKNOWLEDGMENTS

The author would like to thank W. A. Glass for suggesting this research and for his helpful comments throughout the investigation. The help of L. A. Braby on the initial design and construction of the apparatus is appreciated. He is indebted to W. C. Roesch for writing the computer programs for

the solid-angle calculations and to W. C. Roesch and W. E. Wilson for many valuable discussions throughout this research and in preparation of this paper. The author would also like to thank A. K. Edwards for sending drawings of his electrostatic analyzer from which ours was designed and M. E. Rudd for providing a copy of his computer program for the binary-encounter calculations.

\*Paper based on work performed under U. S. Atomic Energy Commission Contract No. AT(45-1)-1830.

<sup>1</sup>C. E. Kuyatt and T. Jorgensen, Jr., *Phys. Rev.* **130**, 1444 (1963).

<sup>2</sup>M. E. Rudd and T. Jorgensen, Jr., *Phys. Rev.* **131**, 666 (1963).

<sup>3</sup>M. E. Rudd, C. A. Sautter, and C. L. Bailey, *Phys. Rev.* **151**, 20 (1966).

<sup>4</sup>H. Hafner, J. Arol Simpson, and C. E. Kuyatt, *Rev. Sci. Instr.* **39**, 33 (1968).

<sup>5</sup>V. V. Zashkvara, M. I. Korsunskii, and O. S. Kosmachev, *Zh. Tekh. Fiz.* **36**, 132 (1966) [*Soviet Phys. Tech. Phys.* **11**, 96 (1966)].

<sup>6</sup>H. Z. Sar-el, *Rev. Sci. Instr.* **38**, 1210 (1967).

<sup>7</sup>A. Egidi, R. Marconero, G. Pizzella, and F. Sperli, *Rev. Sci. Instr.* **40**, 88 (1969).

<sup>8</sup>K. C. Schmidt, Bendix Electro-Optics Division Technical Applications Note 9803, 1969 (unpublished).

<sup>9</sup>S. Dushman, *Scientific Foundations of Vacuum Techniques* (Wiley, New York, 1962).

<sup>10</sup>E. Bar-Avraham and L. C. Lee, University of Southern California Report No. USC-136-138, 1968 (unpublished).

<sup>11</sup>C. E. Normand, *Phys. Rev.* **35**, 1217 (1930).

<sup>12</sup>T. A. Carlson and M. O. Krause, *Phys. Rev. Letters* **17**, 1079 (1966).

<sup>13</sup>A. K. Edwards and M. E. Rudd, *Phys. Rev.* **170**, 140 (1968).

<sup>14</sup>Tabulated cross sections can be obtained from the author upon request.

<sup>15</sup>H. Ehrhardt, M. Schulz, T. Tekaas, and K. Willmann, *Phys. Rev. Letters* **22**, 89 (1969).

<sup>16</sup>D. A. Vroom, Gulf General Atomic Annual Report No. GA 9713, UC-34, 1969 (unpublished).

<sup>17</sup>M. E. Rudd and D. Gregoire, in *Physics of the One- and Two-Electron Atoms*, edited by F. Bopp and H. Kleinpoppen (North-Holland, Amsterdam, 1969), pp. 795-800; M. E. Rudd (private communication).

<sup>18</sup>E. Gerjuoy, *Phys. Rev.* **148**, 54 (1966).

<sup>19</sup>L. Vriens, *Proc. Phys. Soc. (London)* **90**, 935 (1967).

<sup>20</sup>B. B. Robinson, *Phys. Rev.* **140**, A764 (1965).

<sup>21</sup>E. J. McGuire, *Phys. Rev.* **185**, 1 (1969).

<sup>22</sup>E. Mertzbacher and H. W. Lewis, in *Encyclopedia of Physics*, edited by S. Flügge (Springer-Verlag, Berlin, 1958), Vol. 34, pp. 166-192.

## Absolute Excitation Cross Sections of He<sup>+</sup> in 20-100-keV He<sup>+</sup>-He Collisions Using Energy-Loss Spectrometry\*

D. R. Schoonover<sup>†</sup> and John T. Park

*Physics Department, University of Missouri, Rolla, Missouri 65401*

(Received 30 July 1970)

Application of positive-ion energy-loss spectrometry has been extended to include experimental determination of absolute excitation cross sections of ground-state helium ions. Helium ion-atom collisions were studied for impact energies ranging between 20-100 keV, in 10-keV intervals. The data were taken with an apparatus resolution between 0.6-0.8 eV full width at half-maximum (FWHM). Cross sections for transitions from ground state to the second and third principal quantum levels of the ion plotted as a function of impact energy were still rapidly increasing at 100 keV. The cross sections at this energy were  $(1.64 \pm 0.28) \times 10^{-18}$  cm<sup>2</sup> for He<sup>+</sup>(1<sup>2</sup>s<sub>1/2</sub>) → He<sup>+</sup>(n=2) and  $(3.46 \pm 0.45) \times 10^{-19}$  cm<sup>2</sup> for He<sup>+</sup>(1<sup>2</sup>s<sub>1/2</sub>) → He<sup>+</sup>(n=3).

### I. INTRODUCTION

The technique of energy-loss spectrometry is rapidly becoming a major tool for studying elementary collision processes. In electron spectrometry, electron exchange and target transitions can be

studied. In positive-ion energy-loss spectrometry, excitation of the projectile ion can also occur. The relative velocity of approach (rather than the impact energy) is the primary parameter considered when making approximations in theoretical calculations.<sup>1</sup> Therefore, since positive ions are considerably

more massive than electrons, the impact energy remains above the inelastic thresholds down to much lower velocities of approach, providing more strenuous tests for acceptable approximations.

Positive-ion energy-loss spectrometry<sup>2</sup> has recently been applied to proton impact investigation of a monatomic species (helium)<sup>3</sup> and to a diatomic species (nitrogen).<sup>4</sup> A transition has been observed by others<sup>5</sup> in He<sup>+</sup>-He collisions which was attributed to excitation of the incident ion while the target atom remained in its ground state. The resolution, however, was not sufficient to permit accurate determination of the cross section.

The measured He<sup>+</sup>-He impact cross sections for excitation transitions in He<sup>+</sup> are needed for diagnostic evaluations in certain applications, such as controlled thermonuclear research, and in various astrophysical and cosmological phenomena. In the latter, the observation of He<sup>+</sup> spectral lines has indicated the presence of this ion in the ionosphere,<sup>6</sup> as a solar wind component,<sup>7</sup> in the ultraviolet and soft x-ray spectra of the sun,<sup>8</sup> in the recombination-cascade spectrum of solar flares,<sup>9</sup> in stellar spectra,<sup>10</sup> and in the visible and ultraviolet spectra of quasars.<sup>11</sup>

The resolution of the University of Missouri, Rolla (UMR) positive-ion energy-loss spectrometer has recently been sufficiently improved to permit the study of ionic excitation transitions. The absolute excitation cross sections reported here are for transitions in helium ions from ground state to He<sup>+</sup> ( $n=2$ ) and He<sup>+</sup> ( $n=3$ ) in 20–100-keV collisions with neutral ground-state helium atoms.

## II. ANALYSIS OF TRANSITIONS IN PROJECTILE

Energy-loss spectrometry involves detection and analysis of the incident-beam projectiles. As the projectiles traverse the collision region, interacting with the target particles, they undergo a certain amount of angular scattering. However, in marked contrast to the behavior of electron projectiles, heavy particle scattering is confined almost entirely to extremely small angles about the forward direction, with scattering of the projectiles through angles appreciably different from zero being extremely rare.<sup>12</sup> The pronounced concentration of the scattering in the forward direction was illustrated theoretically.<sup>13</sup> These results have been verified experimentally<sup>14–16</sup> by measuring cross sections as a function of angle about the forward direction.

Thus, the projectile beam may be described as being well defined both in and following the interaction region. The cross sections obtained from the UMR positive-ion energy-loss spectrometer, which collects the forward-scattered beam, are differential in energy loss. That is, these cross sections are essentially equivalent to the angular

energy-loss doubly differential cross sections integrated over all angles.<sup>17</sup>

The theory of positive-ion energy-loss spectrometry has been given elsewhere.<sup>18</sup> The following discussion is an extension of that analysis to include transitions in the projectile.

For ion-atom impact collisions, the detected transitions for excitation of the projectile ions are superimposed on the ionization continuum of the atom. Capture-loss cycling, which also appears as a continuum, and energy-loss transitions due to double scattering may also be superimposed on the ionic transitions. However, these various responses are additive.<sup>18</sup> The total background continuum can therefore be suppressed, exposing the ionic transitions for evaluation. The complications due to double scattering can be removed as described below.

The appropriate model for determining energy-loss cross sections for transitions in the projectile is shown in Fig. 1 for the transition  $\sigma_p$ . In this model,  $I_{10}$  represents the monoenergetic unscattered incident-beam current, and  $I_{1p}$  represents the monoenergetic-beam, or partial-beam, current generated by the  $\sigma_p$  transition. In Fig. 1,  $\sigma_c$  represents the cross section for losses of the incident beam due to charge-changing interactions. Also,

$$\sigma'_j \equiv \sigma_j - \sigma_p, \quad (1)$$

where  $\sigma_j$  represents the cross section for all other incident-beam losses. The inelastic collision losses and the charge-changing losses for partial beam  $I_{1p}$  are not identical to those for the incident beam, since some of the projectiles in the former remain in an excited state throughout the remainder of the scattering region. These loss cross sections for partial beam  $I_{1p}$  have an additional subscript to denote these differences ( $\sigma_{ce}$  and  $\sigma_{je}$ ).

The differential equations describing the model in Fig. 1 are

$$dI_{10} = -I_{10}(\sigma_c + \sigma_j) n dx \quad (2)$$

and

$$dI_{1p} = I_{10} \sigma_p n dx - I_{1p}(\sigma_{ce} + \sigma_{je}) n dx, \quad (3)$$

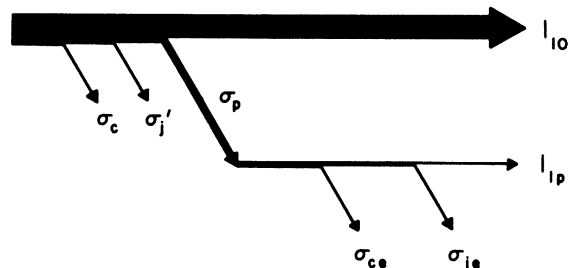


FIG. 1. Simplified partial-beam model for projectile transitions.

where  $n$  is the number density of the target particles and  $dx$  is the differential scattering length measured along the collision path. With the boundary conditions  $I_{1p} = 0$ ,  $I_{10} = (I_{10})_i$  [where  $(I_{10})_i$  is the incident current entering the scattering region] when  $x = 0$ , the solutions of Eqs. (2) and (3) for the beams emerging from the scattering region ( $x = l$ ) are

$$(I_{10})_f = (I_{10})_i e^{-(\sigma_c + \sigma_j)nl} \quad (4)$$

and

$$(I_{1p})_f = [(I_{10})_f \sigma_p / \lambda] (e^{\lambda nl} - 1), \quad (5)$$

where

$$\lambda = (\sigma_c + \sigma_j) - (\sigma_{ce} + \sigma_{je}). \quad (6)$$

If the quantity in Eq. (6) and the target particle density satisfy the "single collision" condition

$$\lambda nl \ll 1, \quad (7)$$

then the exponential in Eq. (5) can be approximated by

$$e^{\lambda nl} \approx 1 + \lambda nl, \quad (8)$$

which permits modification of Eq. (5) to the form

$$\sigma_p = \frac{1}{nl} \frac{(I_{1p})_f}{(I_{10})_f}, \quad \lambda nl \ll 1. \quad (9)$$

Since the approximation in Eq. (8) is mathematically equivalent to the assumption

$$\sigma_c + \sigma_j = \sigma_{ce} + \sigma_{je}, \quad (10)$$

Eq. (9) is identical to the results which are obtained for transitions in the target particles.<sup>18</sup>

To allow for possible differences between  $\sigma_c + \sigma_j$  and  $\sigma_{ce} + \sigma_{je}$  due to excitation of the projectiles, consider the approximation

$$e^{\lambda nl} \approx 1 + \lambda nl + \frac{1}{2} (\lambda nl)^2. \quad (11)$$

Then, from Eq. (5),

$$(I_{1p})_f = (I_{10})_f \sigma_p nl (1 + \frac{1}{2} \lambda nl). \quad (12)$$

For the target pressure region where Eq. (12) is applicable, the  $\sigma_p$  cross section can be determined by least-squares fitting of experimental data for  $(I_{1p})_f / (I_{10})_f$  versus reduced pressure  $p_0$  to an equation of the form<sup>18,19</sup>

$$(I_{1p})_f / (I_{10})_f = ap_0 + bp_0^2. \quad (13)$$

The reduced pressure is related to the target particle density

$$n = N_L p_0, \quad (14)$$

where  $N_L$  is Loschmidt's number

$$N_L = 3.54 \times 10^{13}, \quad (15)$$

which is the number of molecules per  $\text{cm}^3$  of ideal gas per unit reduced pressure. Also,

$$p_0 = (273/T)p, \quad (16)$$

where  $T$  is the absolute temperature in degrees Kelvin, and  $p$  is the target gas pressure in millitorr. Then, from Eqs. (12)–(14),

$$a = \sigma_p N_L l, \quad (17)$$

$$b = \frac{1}{2} \sigma_p N_L^2 l^2 \lambda. \quad (18)$$

Since partial beams due to double scattering vary quadratically with the pressure,<sup>18</sup> these complications are also separated from the linear variation with  $p_0$ . The  $\sigma_p$  ionic-transition cross section, in this approximation, can then be determined by using the linear least-squares constant in Eq. (17).

### III. DESCRIPTION OF APPARATUS AND METHOD OF OPERATION

The University of Missouri, Rolla, 250-kV acceleration-deceleration positive-ion energy-loss spectrometer was used to perform this study. This machine and the associated apparatus have been described in detail elsewhere.<sup>2,18</sup> The following description is a summary of the basic features of the apparatus and the method of operation.

The  $\text{He}^+$  ions were generated in a Colutron<sup>20</sup> ion source by bombarding helium gas with electrons having a maximum energy of 40 eV (below the lowest metastable state in helium ions). The ions extracted from this source had a kinetic-energy distribution of approximately 0.1 eV. These ions were focused by an Einzel lens and were accelerated through a potential  $V$ . The energetic ions then impinged on the target gas which was contained in the center cell of a differentially pumped scattering chamber. The collision region, which had a length of 6.31 cm, was defined by two tantalum disks pierced with 0.051-cm-diam orifices. The pressure of the target gas was monitored with an MKS Baratron<sup>21</sup> 77M-XRP differential pressure meter. A nulling signal from this meter was fed into a servo-amplifier feedback control system which automatically maintained the target gas pressure in the scattering chamber at any desired value.

The beam emerging from the scattering chamber was magnetically mass analyzed. The high-resolution energy analysis of the energy distribution of the emergent beam, which is required in energy-loss spectrometry, was then accomplished by decelerating the ion beam to a low well-defined energy,  $eV_0 = 2$  keV, before entering a 127° electrostatic analyzer. With the analyzer-plate voltage adjusted for maximum signal, the energy-loss spectrum was examined by slowly and continuously increasing the difference between the acceleration-deceleration potentials. This differential voltage  $\Delta V$  was swept over the entire energy-loss range of interest, while maintaining the magnetic mo-

mentum analysis and the electrostatic energy analysis at fixed values.

Due to the kinetic-energy distribution of the incident beam and due to the finite resolving power of the analyzer, a trace obtained without target gas in the scattering chamber,  $\Phi(\xi)$ , was a convolution of the energy spread in the ion beam and the dispersive effects of the apparatus. The magnitude of  $\Phi(\xi)$ , where  $\xi$  was the differential energy loss, was proportional to the beam current. Without altering any other experimental parameters, target gas was introduced into the scattering chamber, and  $\Delta V$  was swept again. The trace then obtained,  $R(\xi)$ , the energy-loss spectrum, was a convolution of the incident-beam energy distribution with the energy and angular effects of the apparatus and of the target gas. The procedure of modifying the accelerating potential by sweeping  $\Delta V$  compensated for the corresponding energy lost in collisions with the target particles. This ensured that all particles reaching the detector had traversed similar trajectories between the scattering chamber and the detector, with energies lying within the same acceptance interval as any other particle reaching the detector. The magnitude of  $R(\xi)$  was proportional to the emergent beam detected with  $n$  atoms/cm<sup>3</sup> of target gas in the scattering chamber.

Typical traces of  $\Phi(\xi)$  and  $R(\xi)$  are shown in Figs. 2(a) and 2(b) for 50-keV He<sup>+</sup> ions incident on helium gas (4 mTorr). The amplified output from the ana-

lyzer is shown as the ordinate and the differential energy loss  $\xi$  as the abscissa. The peak at the left of each trace is due to transmitted and elastically scattered projectiles. The first two essentially resolved peaks in the energy-loss spectrum of Fig. 2(b) correspond to discrete inelastic transitions in the target helium atoms. The discrete peaks superimposed on the ionization continuum of the target particles are excitation transitions in the He<sup>+</sup> projectiles. The mathematical relationship between these two traces  $R$  and  $\Phi$  and inelastic transitions has been described in detail elsewhere.<sup>17</sup> The result of that analysis is briefly outlined below.

Since the two functions  $R(\xi)$  and  $\Phi(\xi)$  were plotted under the same experimental conditions with the introduction of target gas into the scattering chamber being the only distinguishing factor, the following relationship holds:

$$R(\xi) = nl \int \Phi(\xi - \xi') \frac{d\bar{\sigma}(\xi')}{d\xi'} d\xi', \quad (19)$$

where

$$\frac{d\bar{\sigma}}{d\xi} \equiv \int_{\Delta\Omega} \frac{d^2\sigma(\theta, \xi)}{d\Omega d\xi} d\Omega. \quad (20)$$

$d^2\sigma/d\Omega d\xi$  is the doubly differential cross section per unit angle per unit energy loss for scattering into the solid angle  $d\Omega$  and energy-loss interval  $d\xi$ .  $\xi$  is a (positive) energy loss as measured from the most probable energy of the decelerated elastically scattered ion beam.  $\theta$  and  $\Delta\Omega$  are the laboratory scattering angle and the instrumental acceptance solid angle, respectively. Due to the predominant peaking in the forward direction in positive-ion energy-loss spectrometry,<sup>12,17</sup> essentially all of the scattered singly charged projectiles are detected. Then, the experimentally determined cross section is equivalent to the energy-loss differential cross section to the extent that

$$\frac{d\bar{\sigma}(\xi)}{d\xi} = \int_{\Delta\Omega} \frac{d^2\sigma(\theta, \xi)}{d\Omega d\xi} d\Omega = \frac{d\sigma(\xi)}{d\xi}. \quad (21)$$

To determine absolute cross sections, it is necessary to assume that the elastic and inelastic contributions to  $R(\xi)$  are separable. Then, if the transition responsible for a peak in the energy-loss spectrum can be identified, and if  $R(\xi)$  with the background suppressed,  $R'(\xi)$ , drops essentially to zero on each side of the peak, integration of  $R'$  over the peak yields the total cross section for that transition. For example, in the pressure range over which Eq. (9) is applicable, the cross section determined from a peak in the energy-loss spectrum is

$$\sigma_p = \int_{\Delta\epsilon_p} R'(\xi) d\xi / nl \int_{\Delta\epsilon_0} R(\xi) d\xi = \frac{1}{nl} \frac{(I_{10})_f}{(I_{10})_f}, \quad (22)$$

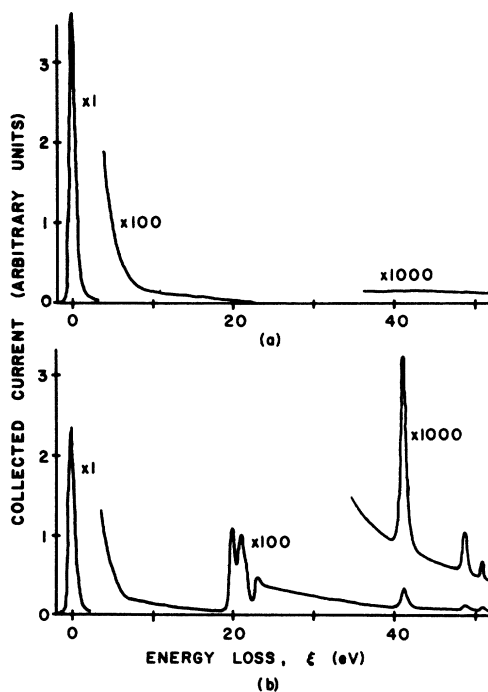


FIG. 2. Energy-loss traces (a) without target gas, and (b) with target gas.

where  $\Delta\xi_p$  is the interval corresponding to the transition peak, and  $\Delta\xi_0$  is the interval corresponding to the elastic and transmitted region of  $R(\xi)$ . The calculated cross sections are "absolute" in the sense that they are not normalized to other data or theory.

#### IV. DATA

The data for this study were taken with helium-ion impact energies ranging between 20–100 keV, in 10-keV intervals. Most of the data were taken with over-all apparatus resolution between 0.6–0.8 eV full width at half-maximum (FWHM). The target thicknesses ranged between 3–50 mTorr cm. The two energy-loss peaks of primary interest were situated at  $40.8 \pm 0.1$  and  $48.4 \pm 0.2$ , which correspond to excitation of the ground-state helium-ion projectiles to the second and third principal quantum levels. As the energy separations between the various states within a quantum level of  $\text{He}^+$  are much too small to be resolved, transitions to the various states within a level contribute to a single peak observed at the energy loss corresponding to the excitation energy of this level above the ground state of the helium ion.

To calculate the cross sections for these two transitions at a given energy, it was necessary to suppress the background continuum, which results primarily from ionization of target He atoms. The background for each transition was obtained by drawing in a baseline which smoothly joined the background on each side of the peak. This background was then subtracted, exposing the peak for cross-section evaluation. To subtract off the continuum in this manner, it must be assumed that the background in the absence of the ionic transitions is slowly varying, containing no structure. The ionization continuum of the helium target gas and the capture-loss continuum satisfy this criterion. The possibility of structural transitions superimposed on the continuum at the location of the ionic transitions can arise primarily from two possible sources: (i) double scattering, and (ii) autoionizing transitions. The double-scattering complication

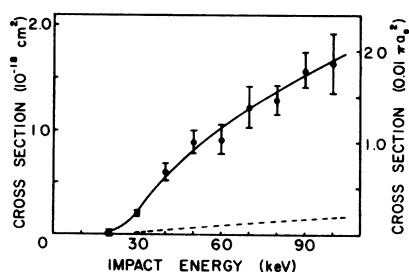


FIG. 3. Solid line: absolute  $\text{He}^+(1^2s_{1/2}) \rightarrow \text{He}^+(n=2)$  ionic transition cross section as a function of impact energy on atomic helium. Dashed line:  $\text{He}^+(1^2s_{1/2}) \rightarrow \text{He}^+(n=3)$  ionic transition cross section.

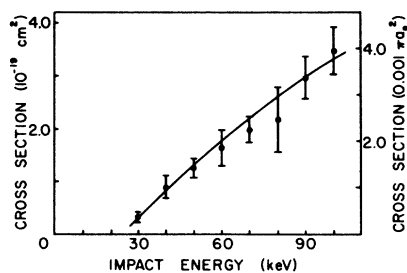


FIG. 4. Absolute  $\text{He}^+(1^2s_{1/2}) \rightarrow \text{He}^+(n=3)$  ionic transition cross section as a function of impact energy on atomic helium.

is removed by the quadratical least-squares fitting of the data as discussed above. The lowest autoionizing energy-loss transition occurs for  $\text{He}(1s^2)^1S \rightarrow \text{He}(2s^2)^1S$  at 57.9 eV.<sup>22</sup> This is sufficiently remote from the energy loss corresponding to the two ionic transitions measured in this experiment that disturbances due to autoionizing transitions are nonexistent. But, if a target particle should be excited by a projectile and then, while still excited, undergo another excitation into an autoionizing level by a collision with a second projectile, the energy loss of this second collision could be superimposed on the detected ionic transitions. However, the scattering density for interactions between projectiles and other collision products is less than  $10^{-8}$  of those for interaction with the target particles themselves.<sup>18</sup> The disturbing influence from the appearance potentials of autoionizing levels therefore can be neglected.

Cross sections for excitation of helium ions to  $\text{He}^+(n=2)$  and  $\text{He}^+(n=3)$  in collisions with helium atoms have been calculated by the method outlined above. These cross sections are shown in Figs. 3 and 4 as a function of impact energy. (The smooth curve sketched through the values plotted in Fig. 4 has been reproduced in Fig. 3 to permit comparison of magnitudes). The error bars shown are vectorial additions (rms values) of the random standard deviations obtained from the least-squares analyses and of an estimated maximum systematic error of 10%, which was largely due to estimated uncertainty in the pressure measurements. These cross sections plotted as a function of impact energy are still rapidly increasing at 100 keV. Within the limits prescribed by the error bars, it appears that the peaks for these curves are situated well above 100 keV. The measurement of cross sections of this order of magnitude ( $\sim 10^{-20} \text{ cm}^2$ ) extends the technique of positive-ion energy-loss spectrometry until it encompasses most of the range covered by experiments observing secondary emission.

In some of the energy-loss data, transitions of the ground-state helium-ion projectiles to the fourth

and fifth principal quantum levels were also resolved. The statistics for these transitions were not sufficient to report calculated cross sections; however, the  $n^{-3}$  law<sup>23</sup> did not appear to be obeyed for excitation to these lower levels in the helium ion.

#### V. DISCUSSION

To the author's knowledge, there are no existing theoretical calculations or experimental determinations with which to directly compare the results of this study. Complete analytical calculations for making a comparison are nonexistent because of the impossibility of obtaining exact solutions for atomic collision cross sections. For any atom more complex than hydrogen, the wave functions are only approximately known, and are frequently nonorthogonal. Further, the complexity of the equations is such that approximate methods must be employed even if the exact wave functions were known. Also, the commonly applied approximations are not really valid for  $\text{He}^+$  projectiles in the impact energy range covered in this study.

A few experiments have been performed for evaluating the characteristics of quantum excitations in helium ions. In particular, a crossed-beam method has been used to measure the cross section of  $\text{He}^+(1s) \rightarrow \text{He}^+(2s)$  by electron impact for energies ranging from threshold to 750 eV.<sup>24</sup> The results of this experiment showed that, at the higher energies, the energy dependence of the cross section is in close agreement with that calculated by means of the plane-wave Born approximation. Most other studies concerning  $\text{He}^+$  have involved simultaneous excitation ionization of helium atoms by electron or proton impact.<sup>25</sup>

As mentioned earlier, ionic excitation transitions have been observed by Boudon *et al.*<sup>5</sup> for  $\text{He}^+$  impacting with He. These experiments were performed with a maximum impact energy of 3 keV. The published data showing the ionic transition were

for the scattered beam collected at  $3^\circ$  from the forward direction. Boudon *et al.* claimed that a collision in which the ion becomes excited while the atom remains unexcited seems very improbable. Looking at Figs. 3 and 4, ionic excitation transitions for the  $\text{He}^+$ -He system are quite probable for impact energies above 20 keV. However, if the curves in Figs. 3 and 4 were extrapolated backward into the energy region covered by the experiments of Boudon *et al.*, the cross sections, even for total scattered current, are indeed very small, probably less than  $10^{-20}$  cm<sup>2</sup>.

Technically, the cross sections determined in this study probably could be measured using crossed-beam techniques. However, absolute measurements using crossed beams would be difficult.

Radiative transitions following  $\text{He}^+$ -He collisions from levels of  $\text{He}^+$  ( $n=3$ ) to levels of  $\text{He}^+$  ( $n=2$ ) should be measurable with ultraviolet spectroscopy. Although the correlation would be indirect, it would be interesting to compare such optical emission measurements with these measurements obtained by energy-loss spectrometry.

It is hoped that the experimentally determined cross sections obtained in this study will provide new insight into currently observed physical phenomena and will contribute to the advancement of the theoretical investigations of atomic structures as embodied in collision cross sections.

#### ACKNOWLEDGMENTS

The authors would like to express their thanks to George York, Victor Pol, and Eugene Aufdembrink for their technical assistance, and to other members of the UMR Physics staff for their cooperation and helpful suggestions. The authors are also very grateful for the Research Corporation Grant which initiated this research project and for the continued support of the National Science Foundation.

\*Work supported by a grant from the National Science Foundation.

†Present address: Corning Glass Works, Bradford, Penn. 16701.

<sup>1</sup>D. R. Bates, *Atomic and Molecular Processes* (Academic, New York, 1962), p. 549.

<sup>2</sup>J. T. Park and F. D. Schowengerdt, *Rev. Sci. Instr.* **40**, 753 (1969).

<sup>3</sup>J. T. Park and F. D. Schowengerdt, *Phys. Rev.* **185**, 152 (1969).

<sup>4</sup>F. D. Schowengerdt and J. T. Park, *Phys. Rev. A* **1**, 848 (1970).

<sup>5</sup>J. Boudon, M. Barat, and M. Abignoli, *J. Phys. B* **1**, 1083 (1968).

<sup>6</sup>E. J. R. Maier, *J. Geophys. Res.* **74**, 815 (1969).

<sup>7</sup>S. J. Bame, A. J. Hundhausen, J. R. Asbridge, and I. B. Strong, *Phys. Rev. Letters* **20**, 393 (1968).

<sup>8</sup>B. B. Jones, F. F. Freeman, and R. Wilson, *Nature* **219**, 252 (1968).

<sup>9</sup>H. Zirin and L. W. Acton, *Astrophys. J.* **148**, 501 (1967).

<sup>10</sup>W. L. W. Sargent and L. Searle, *Astrophys. J.* **152**, 443 (1968).

<sup>11</sup>C. Lari and G. Setti, *Nuovo Cimento* **B52**, 507 (1967).

<sup>12</sup>E. W. McDaniel, *Collision Phenomena in Ionized Gases* (Wiley, New York, 1964), p. 284.

<sup>13</sup>H. S. W. Massey and R. A. Smith, *Proc. Roy. Soc. (London)* **A142**, 142 (1933).

<sup>14</sup>Q. C. Kessel and E. Everhart, *Phys. Rev.* **146**, 1524 (1965).

<sup>15</sup>V. V. Afrosimov, Yu. Gordiev, M. Panov, and N. V. Fedorenko, *Zh. Tekhn. Fiz.* **36**, 123 (1966) [*Soviet Phys. Tech. Phys.* **11**, 89 (1966)].

<sup>16</sup>M. Barat and J. C. Houver, *Compt. Rend.* **264B**,

38 (1967); 264B, 296 (1967).

<sup>17</sup>For a detailed discussion, see F. D. Schowengerdt, Ph. D. dissertation, University of Missouri, Rolla, 1969 (unpublished).

<sup>18</sup>D. R. Schoonover, Ph. D. dissertation, University of Missouri, Rolla, 1970 (unpublished).

<sup>19</sup>The procedure for least-squares fitting experimental data to a mathematical function is given by Yardley Beers, *Introduction to the Theory of Error* (Addison-Wesley, Reading, Mass., 1957), pp. 38-43.

<sup>20</sup>Colutron Corporation, Boulder, Colo.

<sup>21</sup>MKS Instruments, Inc., Burlington, Mass.

<sup>22</sup>J. Arol Simpson, G. E. Chamberlain, and S. R. Mielczardk, *Phys. Rev.* 139, A1030 (1965).

<sup>23</sup>V. I. Ochkur and A. M. Petrunin, *Opt. i Spektroskopiya* 14, 457 (1963) [*Opt. Spectry. (USSR)* 14, 245 (1963)].

<sup>24</sup>D. F. Dance, M. F. A. Harrison, and A. C. H. Smith, *Proc. Roy. Soc. (London)* A290, 74 (1966).

<sup>25</sup>See, for example, H. R. Moustafa Moussa and F. J. DeHeer, *Physica* 36, 646 (1967).

PHYSICAL REVIEW A

VOLUME 3, NUMBER 1

JANUARY 1971

## Faddeev Approach to the Ground State of Three-Particle Coulomb Systems\*

S. Radhakant

*Tata Institute of Fundamental Research, Colaba, Bombay 5, India*

and

C. S. Shastry and A. K. Rajagopal<sup>†</sup>

*Department of Physics and Astronomy, Louisiana State University, Baton Rouge, Louisiana 70803*

(Received 15 April 1970)

Using a one-state approximation in the Faddeev equations, the ground-state energies of several three-particle Coulomb systems are computed and compared with the earlier variational results. The simplicity and general applicability of this method are in contrast with the variational techniques. Our results also give an idea of the accuracy involved in a one-state approximation for the Faddeev kernel. Some major numerical difficulties are illustrated. Complete analytical expressions for the Faddeev kernel in the two-state approximation are given in an appendix.

### I. INTRODUCTION

This paper contains the results of the calculations of the ground-state energies of several interesting three-particle Coulomb systems using the Faddeev formulation of the three-body problem<sup>1,2</sup> in the one-state approximation. In contrast with the various variational techniques developed for these systems only a decade ago, this approach is novel and rigorous in principle. The computations involved are not variational. A single simple analytical expression for the Faddeev kernel for three-particle Coulomb systems can be obtained in the one-state approximation.<sup>3</sup> This is a general expression valid for all finite masses and charges, and therefore the evaluation of the bound states of a large number of three-particle Coulomb systems becomes straightforward. It is this unique feature which motivated us to pursue the present work. The Faddeev approach is exact when all the states are included. But this is clearly impossible to achieve at present in a practical computation. We chose to employ a one-state approximation as a first try. The higher states can in principle be incorporated, but a glance at the Appendix shows that the numerical evaluation very quickly becomes formidable. It may be ar-

gued that, without a knowledge of the convergence of the calculation as more and more states are included, the results obtained may at best be fortuitous. On physical grounds, the status of the one-state approximation in the Faddeev theory may be compared with early variational calculations which employed the hydrogenic ground-state wave function as a trial solution. The inclusion of all the higher states makes the Faddeev theory *exact*; the contribution from higher states to what is obtained in the one-state scheme may therefore be safely stated to amount to about 15% at best, this being the worst deviation from the best-known variational result (except  $pe^+e^-$ ). We have not addressed ourselves here to the question of obtaining the best numerical value for the ground state, but of seeking a "workable approximation" scheme. The problem of convergence is a separate one.

Here we report the ground-state energies of various three-particle Coulomb systems obtained by this method and compare them with the corresponding variational results. The difficulties in performing these computations – in particular, for arbitrary masses – will be illustrated. These difficulties make evaluation of ground-state energies by the Faddeev method somewhat unreliable at the present